

# Microstructure analysis of mangan ferrite synthetic (XRD, DTA, SEM) using citric acid surfactant

Rini Anggraini<sup>1</sup>; Rita Sundari<sup>1\*</sup>; Popy Yuliarty<sup>2</sup>

Department of Mechanical Engineering, Universitas Mercu Buana, Jakarta 11650<sup>1</sup>

Department of Industrial Engineering, Universitas Mercu Buana, Jakarta 11650<sup>2</sup>

corresponding author: [sundaririta15@gmail.com](mailto:sundaririta15@gmail.com)<sup>1\*</sup>; [rita.sundari@mercubuana.ac.id](mailto:rita.sundari@mercubuana.ac.id)<sup>1\*</sup>

## ABSTRACT

*This investigation has studied the microstructure analysis of mangan ferrite synthesized by sol gel route applying citric acid anionic surfactant followed by calcinations (300°C, 600°C, and 800°C). The XRD (X-Ray Diffraction) spectra showed that crystallization formation of Mn-ferrite beginning at calcinations of 300°C - 600°C. The XRD spectra showed that at 300°C calcinations the Mn-ferrite was still in large part of brittle amorphous structure. The DTA-TGA (Differential Thermal Analysis-Thermal Gravimetric Analysis) analysis investigated endothermic peak of H<sub>2</sub>O removal followed by mixture of CO, CO<sub>2</sub>, and NO<sub>x</sub> gasses removal for 100°C sol gel matrix, while at calcinations of 600°C showed a flat line attributed to no more volatile matter removal. The SEM (Scanning Electron Microscope) mapping of Mn-ferrite with regard to Mn distribution at varied calcinations temperature (300°C, 600°C, and 800°C) and 100°C (sol gel form) yielded indifferent profiles, however, the EDX (Energy Dispersive X-Ray) patterns integrated to SEM showed a fluctuation of Mn and Fe atomic concentrations by altering heat temperature due to oxidation numbers of Mn transition elements. It should be noted that fabricated Mn-ferrite (mangan ferrite) has remarkable electrical and magnetic properties for manufacturing of semiconducting materials.*

**Keywords:** DTA; calcinations; Mn-ferrite; SEM; sol gel; XRD.

## 1. INTRODUCTION

Mn-ferrite (mangan ferrite) has many broad applications in various fields due to its remarkable magnetic properties such as reagent for MRI (Magnetic Resonance Imaging), magnetic recording, drug

transportation and ferrous liquid, as well as biosensor [1]. In general, ferrite material is highly resistant to very high temperature, therefore, many ferrite compounds as ceramic material have been used as component mixture in refractory for fusion mining ores at high temperature. Although Mn-ferrite has been found in natural ferrite mixture, however, the separation process of Mn-ferrite from its complex ferrite mixture requires elaborate procedure and yields low grade Mn-ferrite. Therefore, the synthesis process of Mn-ferrite in lab-scale is often done to produce high grade mangan ferrite. There are several methods to synthesize Mn-ferrite. Sol gel route is the common method to synthesize Mn-ferrite due to its simple process beside co-precipitation and hydrothermal methods [2]. Innocenzi et al. [3] reported sol gel method was used for synthesis of nano filtration membrane until nano level (< 5 nm). The sol gel route was also developed for synthesis of aptamer DNA membrane made of silica material [4] and for yielding ceramics matrix to immobilize *subtilisin* used in synthesis of paint protector [5]. Depending on the synthesis method and atomic arrangement in crystal lattice the mangan ferrite synthetic may have chemical structure as MnFeO<sub>3</sub> (*perovskite* ferrite) or MnFe<sub>2</sub>O<sub>4</sub> (*spinel* ferrite). At broad scale Mn-ferrite has been produced through sintering technique of amorphous solid like processing of ferromagnetic material at high temperature via calcinations [6]. The optimization of mole ratio between Mn and Fe is needed to ensure the level of product purity. In general, silica impurities are often found in the production of mangan ferrite from natural ferromagnetic ores. In order to examine the Mn-ferrite crystal structure there are several microstructure analyses such as FTIR (Fourier Transformation Infra Red), XRD (X-Ray Diffraction), DTA-TGA, SEM mapping with EDX detector, FESEM (Field Emission Scanning Electron Microscope) and TEM (Transmission Electron Microscope). On account of this reason, this study attempts to synthesize Mn-ferrite using sol gel route

applying citric acid as anionic surfactant. The synthesis is accomplished by calcinations at varied temperatures (300°C, 600°C, and 800°C). Analysis of microstructure has done for XRD, DTA-TGA, and SEM-EDX. The XRD analysis was conducted to examine the amorphous/crystalline structure of Mn-ferrite and the existence of other impurities during calcination process. The DTA-TGA analysis was done to examine the endothermic reaction of volatile matter removal during change of heat supplies. The SEM analysis was applied to survey the surface morphology of synthetic material with EDX as the detector to report the atomic distribution on the surface part.

## 2. MATERIAL AND METHOD

This investigation applied  $\text{MnO}_2$  (Merck) and  $\text{Fe}(\text{NO}_3)_3 \cdot 9\text{H}_2\text{O}$  (OReC) as precursors. The citric acid ( $\text{C}_6\text{H}_8\text{O}_7 \cdot \text{H}_2\text{O}$ ) (OReC) as anionic surfactant was needed to assist the sol gel process at moderate temperature. All chemicals are in analytical grade. The mole ratio between precursors affects the product quality in terms of purity and therefore, optimization of chemicals concentration in sol gel method is necessary. The sol gel method used in this study was adapted from previous procedure for the synthesis of magnesium ferrite [7]. The procedure applied can be summarized as follows: (i) All chemical materials (manganese oxide + iron nitrate anhydrous + citric acid) are dissolved in distilled water using a glass container. (ii) The mixture was heated at 60°C for 3h with constant stirring using a magnetic pin. (iii) The temperature was increased to 80°C with constant stirring until sol gel formation. (iv) The solution gel was dried at 100°C for 24h in an oven. (v) After dried, calcinations was conducted in a muffle furnace at varied temperatures (300°C, 600°C, and 800°C) for 2h, respectively. (vi) Characterizations of synthetic material were done for XRD, DTA-TGA, and SEM-EDX, respectively. The XRD instrument used in this study has specifications as follows: Philips XL 40, with anode CuK $\alpha$  1 radiation, 30 mA current, 40 kV voltage, and wavelength of 1.5406 nm scanning for  $2\theta = 10^\circ - 80^\circ$ . This study used the DTA-TGA thermal analyzer (Mettler-Toledo) with heating rate 10°C – 20°C/min up to 100°C/min at operating range of -200°C – 1600°C) and inert  $\text{N}_2$  purging gas. The incorporated EDAX analysis and SEM mapping (JEOL) was applied to obtain the atomic distribution on ferrite surface with magnification image is up to 30 000 for backscattered electrons imaging mode and 25 kV voltage.

## 3. RESULTS AND DISCUSSION

### 3.1 XRD Analysis

The results of XRD analysis yielded diffractograms at varied calcination temperatures (300°C, 600°C, and 800°C) and the sol gel matrix at 100°C (Fig.1). Moreover, the XRD diffractograms (Fig.1) for mangan ferrite show that the transition phase from amorphous to crystalline structure occurred in the temperature range of 300°C-600°C. The sharp peaks of diffractogram as shown in calcination of 800°C attributed to crystalline structure of mangan ferrite. On the other hand, the flat pattern of calcination (300°C) attributed to amorphous solid. The quantity of peaks indicated the degree of crystalline structure as the “800°C” showed higher degree crystalline structure compared to that of “600°C”. It is in agreement with the fact that the higher calcinations temperature gives more chance for atomic distribution and arrangement to form more perfect crystalline structure. Thus, the calcinations effect is strongly related to change in material structure from amorphous through semi crystalline to high degree crystalline structure. According to Hu et al. [8] the size of nano mangan ferrite at  $2\theta = 35^\circ$  are about 36, 45, and 16 nm depending on the methods used for synthesis of mangan ferrite (co-precipitation, sol-gel, and hydrothermal). There is a similarity between this study and the report of Zipare et al. [9] in terms of (400) and (440) planes in the X- ray diffractogram of mangan ferrite indicated super paramagnetic characters of mangan ferrite crystalline structure. Zipare et al. [9] used co-precipitation method and found the crystalline structure of mangan ferrite as  $\text{MnFe}_2\text{O}_4$ , while this study used sol gel method and found the structure as  $\text{MnFeO}_3$ . According to Zipare et al. [9] the peak width of (311) plane is an indication of mangan ferrite in nano size. Based on the report of Deraz and Alafiri [10]  $\text{MnFe}_2\text{O}_4$  has *spinel* structure with 80% of Mn(II) in tetrahedral position and 20% of Mn(II) in octahedral position. Thus, the nano size of  $\text{MnFe}_2\text{O}_4$  has strong anisotropic character and high Curie temperature causing mangan ferrite is necessary for semiconducting material fabrication.

### 3.2 DTA-TGA Analysis

The thermal analysis will show the heat change of endothermic or exothermic reaction occurred during calcinations process. A coupling of DTA and TGA analyzer was applied to examine the change of crystal structure due to change of temperature (DTA) yielding decomposition reaction and the change of mass due to change of heat in relation to chemical reaction such as

removal of volatile matter, chemical bond breakage, and oxidation-reduction process. Fig. 2 illustrates the TGA profile (upper part) and DTA pattern (lower part). The TGA profile describes the correlation

between mass change (% weight) due to chemical reactions and heating rate of 10°C/min. The DTA pattern describes the correlation between differential temperature (dQ/dT) and heating rate of 10°C/min.

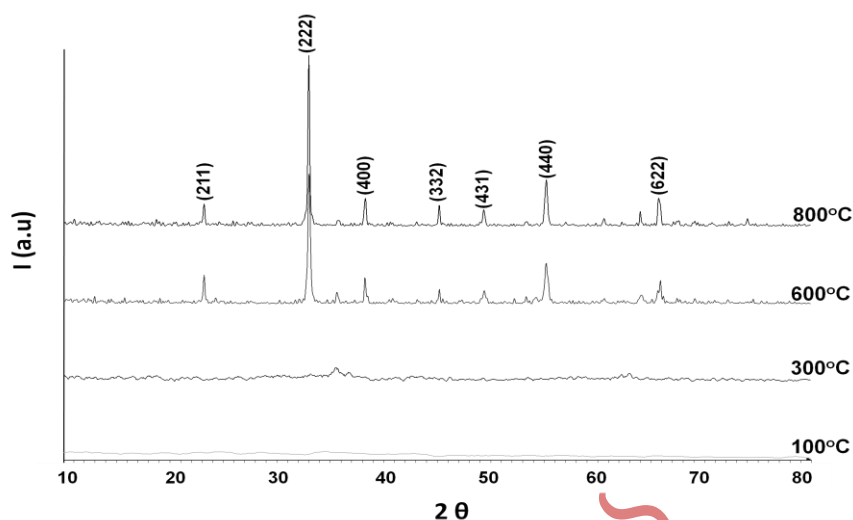


**Fig 1: XRD patterns of mangan ferrite synthetic at varied temperatures (100°C, 300°C, 600°C, and 800°C). Sol gel route with citric acid.**

Furthermore, there are two deflection points (“1” and “2”) in TGA (Fig. 2). The point “1” refers to breaking cohesive bonds due increasing temperature yielding water molecule (H<sub>2</sub>O) removal from the sol gel matrix (100°C). At 100°C the matrix is still in sol gel form and contains a quantity of water molecules attributed to endothermic peak in DTA profile related to endothermic water removal reaction and illustrated as deflection point “1” in TGA pattern. The deflection point “1” for sol gel form at 100°C indicated a mass reduction related to removal of water molecules. The second deflection point (point “2”) of the sol gel at 100°C in TGA profile indicated a reduction of mass (100°C) due to accumulated removal of CO, CO<sub>2</sub> and NO<sub>x</sub> gasses at higher heating rate attributed to endothermic broader peak illustrated in DTA profile. Either the water removal or the accumulated gasses release (CO, CO<sub>2</sub>, and NO<sub>x</sub>) required heat energy obtained from increasing heating rate. The peak height and width is proportional with the concentration of volatile matter in the matrix. The removal of CO and CO<sub>2</sub> gasses are probably comes from citric acid as anionic surfactant, while the NO<sub>x</sub> gasses comes from break down reaction of Fe(NO<sub>3</sub>)<sub>3</sub>. H<sub>2</sub>O precursor. On the other hand, at the calcinations of 600°C, all volatile matters loss and both the DTA and TGA profiles showed a flat line indicated no more mass reduction and endothermic reaction. Therefore, the given range of

heating rate up to 70°/min yielded no effect either on mass reduction or chemical reaction.

### 3.3 SEM Analysis

SEM analysis is related with collision between electron and material in order to get information about atomic distribution on matter surface. The grayscale image of the matter obtained from the backscattered or secondary electrons using a very high magnification. The SEM analysis is usually in coupling with EDX device as the detector to provide signal information.

**Table 1. Atomic distributions of Mn-ferrite resulted from EDX analysis. Mn-ferrite synthesis using citric acid anionic surfactant. Calcinations at 300°C, 600°C, 800°C.**

Temp (°C)	Mn (wt%)	Fe (wt%)	O (wt%)	C (wt%)
100	22.89	22.21	24.14	30.76
300	30.33	30.25	16.18	23.24
600	18.97	18.46	19.30	43.27
800	27.92	26.83	17.01	28.23

Table 1 shows a balancing of atomic distribution between manganese and iron for each given temperature (100°C, 300°C, 600°C, and 800°C). The atomic weights of Mn and Fe are about 54.94 and

55.85 g/mole, respectively, thus, the interaction forces between Mn and Fe are almost equal. In addition, the ionic radii of Mn(III) and Fe(III) are 78.5 picometer ( $1 \text{ pm} = 10^{-12} \text{ m}$ ), respectively. Therefore, the probability

of Mn (III) and Fe(III) ions to occupy crystal lattice are balanced and the chemical structure is likely as  $\text{MnFeO}_3$  *perovskite* instead of  $\text{MnFe}_2\text{O}_4$  *spinel* structure.

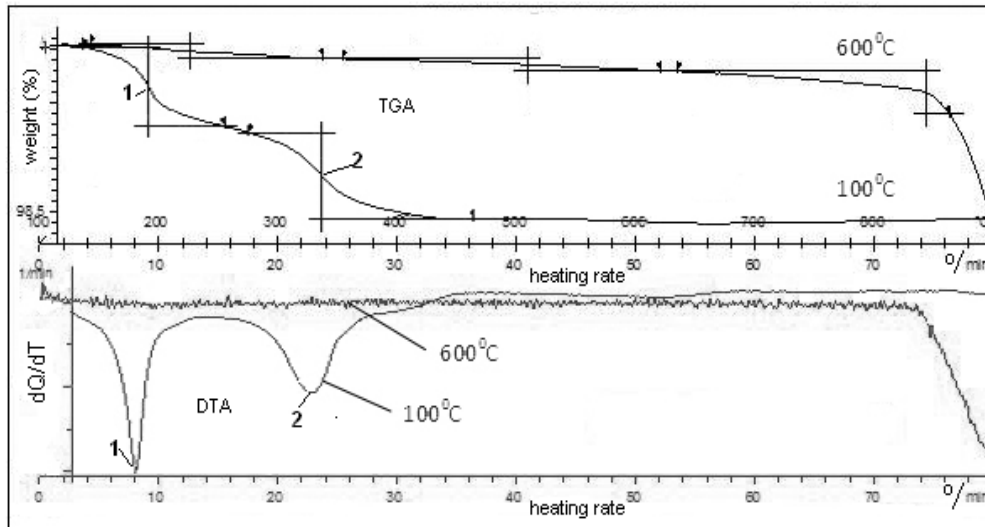


**Fig. 2** DTA-TGA patterns of Mn-ferrite synthetic at 100°C and 600°C. Sol gel method with citric acid. DTA pattern (lower part). TGA pattern (upper part).

From the atomic distribution in crystal lattice, the  $\text{MnFeO}_3$  cubic *perovskite* is more flexible than the *spinel* structure of  $\text{MnFe}_2\text{O}_4$ . Since the  $\text{MnFeO}_3$  is referred to *perovskite* ferrite, it gives more flexibility for oxygen diffusion as shown by the drift of oxygen concentration in Table 1. It is expected that the carbon element may obtain from reduction reaction at higher temperature (600°C and 800°C) and from organic compound (residue of citric acid) at lower temperature (100°C and 300°C).

By glance view, it seems that at higher temperature (600°C) the profile of Mn atoms looks more crowded than its profile at lower temperature (100°C) as demonstrated by SEM mappings in Fig. 3(a) and Fig. 3(c). Regarding to this phenomenon the thermal effect gave more repulsion force to Mn atoms going to surface due to volume expansion.



(a) 100°C



(b) 300°C

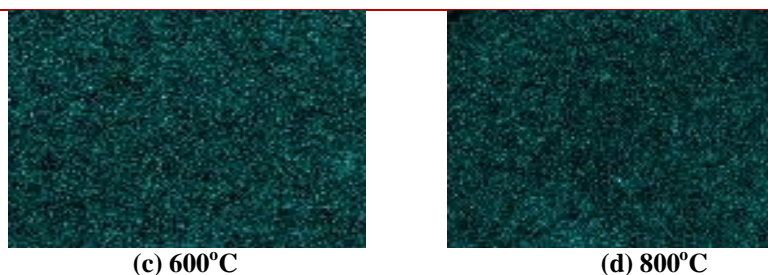


**Fig. 3 SEM of Mn-ferrite synthetic with Mn distribution at varied temperatures (100°C, 300°C, 600°C, and 800°C). Sol gel route with citric acid. 25.0 kV. 500x magn.**

#### 4. CONCLUSION

The study gives valuable information for manufacture of remarkable semiconducting ferrites considering synthesis route, elemental composition, reagent selection, and variable conditions to manage the desired product quality. The characterizations of ferrite material with regard to XRD, DTA-TGA, and SEM mappings-EDX detection are necessary for studying manganese ferrite properties related to *perovskite* and *spinel* structures.

#### 5. ACKNOWLEDGMENTS

The authors give special appreciation to Universitas Mercu Buana, Jakarta for research funding. Several parts of laboratory work have been conducted in UTM Skudai, Johor Bahru, Malaysia.

#### 6. REFERENCES

- [1] M.G.Naseri, E.B.Saion, H.A.Ahangar, M.Hashim, and A.H. Shaari. "Synthesis and Characterization of Manganese Ferrite Nanoparticles by Thermal Treatment Method", *Magnetism and Magnetic Materials*, 323, pp.1745-1749, 2011.
- [2] R. Sundari, I.H.Tang, and R.Yosfiah. "Effect of calcinations on characterizations of fabricated nano manganese ferrite", *Advanced Materials Research*, 634-638, pp.2150-2154, 2013.
- [3] P.Innocenzi, Y.L. Zub, and V.G. Kessler. "Sol-gel approaches in the synthesis of membrane materials for nanofiltration and pervaporation", *Sol Gel Methods for Materials Processing*, Springer Science BV, pp. 47-65, 2008.
- [4] Y.H.Christy, Y.Li, and J.D. Brennan. "Fluorescence analysis of the properties of structure-switching DNA aptamers entrapped in sol gel derived materials", *Chemistry of Materials*, 26, pp.1896-1904, 2014.
- [5] V.R.Regina, S.Helmer, A.R.Lokanath, B.Claus, K. Peter, P.R.Niels, and R.L. Meyer. "Entrapment of subtilisin in ceramic sol-gel coating for antifouling applications", *Applied Materials & Interfaces*, 4, pp.5915-5921, 2012.
- [6] Y.M.Z.Ahmed. "Synthesis of manganese ferrite from non-standard raw materials using ceramic technique", *Ceramics International*, 36, pp.969-977, 2010.
- [7] I.H.Tang, and R Sundari. "Fabrication and characterization of ferrites (Mg and Mn) based on FTIR, XRD, SEM and TEM", *Malaysian Journal of Fundamental and Applied Sciences*, 8, pp.149-154, 2012.
- [8] H.Hu, Z.Tian, J.Liang, H.Yang, A. Dai, L.An, H.Wu, and S Yang. "Surfactant controlled morphology and magnetic property of manganese ferrite nanocrystal contrast agent", *Nanotechnology*, 22, pp.1-7, 2011
- [9] K.J.Zipare, S. Dhumal, V.Bandgar, Mathe, and G Shahane. "Superparamagnetic manganese ferrite nanoparticles: Synthesis and magnetic properties", *Journal of Nanoscience and Nanoengineering*, 1, pp.178-182, 2015.
- [10] N.M.Deraz, and A Alarifi. "Controlled synthesis, physicochemical and magnetic properties of nanocrystalline Mn ferrite system", *International Journal of Electrochemical Science*, 7, pp.5534-5543, 2012.
- [11] S.Alva, T.I.Hua, U.K.Nizar, H.Wahyudi, and R Sundari. "Sol gel method for synthesis of semiconducting ferrite and the study of FTIR, DTA, SEM and CV". *IOP Conf.Series: Materials Science and Engineering*, 343, 012002, 2018.
- [12] R.Sundari, S.Alva, D.Sebayang, H.Wahyudi, S.Jonit, and A. Kamaruddin. "Characterization of fabricated MnO<sub>2</sub>-amberlite photocatalyst by FTIR, XRD and SEM for alizarin removal". *IOP Conf.Series: Materials Science and Engineering*, 343, 012003,2018.